



Optimal Approximation of Fractional Order Brain Tumor Model Using Generalized Laguerre Polynomials

Z. Avazzadeh¹ · H. Hassani² · M. J. Ebadi³ · P. Agarwal^{2,6,7,8} · M. Poursadeghfard⁴ · E. Naraghirad⁵

Received: 1 August 2022 / Accepted: 18 November 2022 / Published online: 4 February 2023
© The Author(s), under exclusive licence to Shiraz University 2023

Abstract

A brain tumor occurs when abnormal cells form within the brain. Glioblastoma (GB) is an aggressive and fast-growing type of brain tumor that invades brain tissue or spinal cord. GB evolves from astrocytic glial cells in the central nervous system. GB can occur at almost any age, but the occurrence increases with advancing age in older adults. Its symptoms may include nausea, vomiting, headaches, or even seizures. GB, formerly known as glioblastoma multiforme, currently has no cure with a high rate of resistance to therapy in clinical treatment. However, treatments can slow tumor progression or alleviate the signs and symptoms. In this paper, a fractional order brain tumor model was considered. The optimal solution of the model was obtained using an optimization method based on operational matrices. The solution to the problem under study was expanded in terms of generalized Laguerre polynomials (GLPs). The study problem was shifted to a system of nonlinear algebraic equations by the use of Lagrange multipliers combined with operational matrices based on GLPs. The analysis of convergence was discussed. In the end, some numerical examples were presented to justify theoretical statements along with the patterns of biological behavior.

Keywords Brain tumor · Glioblastoma multiforme · Generalized Laguerre polynomials · Optimization method

Mathematics Subject Classification 97M60 · 41A58 · 92C42

✉ H. Hassani
hossein hassani40@yahoo.com;
hossein.hassani@anandice.ac.in

Z. Avazzadeh
avazzadz@unisa.ac.za

M. J. Ebadi
ebadi@cmu.ac.ir

P. Agarwal
praveen.agarwal@anandice.ac.in;
goyal.praveen2011@gmail.com

M. Poursadeghfard
poursadegh@sums.ac.ir

E. Naraghirad
esnaraghirad@yu.ac.ir

1 Introduction

Glioblastoma multiform (GBM) is the most frequent malignant brain tumor which accounts for 16% of primary central nervous system (CNS) tumors (Thakkar et al. 2014). Although GBM mainly occurs in the brain, it can rarely appear in the brain stem, cerebellum, or spinal cord (Blissitt 2014). GBMs are derived from glial cells in the CNS; however, other neural stem cells may serve as the cell of origin for gliomas (Phillips et al. 2006).

The median age of GBM is diagnosed at 64 years (Thakkar et al. 2014), but it can also affect patients at different ages even children. Except for higher proliferative

¹ Department of Mathematical Sciences, University of South Africa, Florida, South Africa

² Anand International College of Engineering, Agra Road, Jaipur, Rajasthan 303012, India

³ Department of Mathematics, Chabahar Maritime University, Chabahar, Iran

⁴ Clinical Neurology Research Center, Shiraz University of Medical Sciences, Shiraz, Iran

⁵ Department of Mathematics, Yasouj University, Yasouj, Iran

⁶ International Center for Basic and Applied Sciences, Jaipur 302029, India

⁷ Peoples' Friendship University of Russia (RUDN University), 6 Miklukho-Maklaya St, Moscow 117198, Russian Federation

⁸ Nonlinear Dynamics Research Center (NDRC), Ajman University, Ajman, UAE

activity of glioma cells in childhood, other morphological features do not differ between adults and children. The incidence rate of this tumor is 1.6 times higher in adult men than women (Ellor et al. 2014; Urbańska et al. 2014).

Some environmental risk factors associated with brain tumors are assumed to be ionizing radiation, smoking, synthetic rubber manufacturing, petroleum refining, air pollution, and toxic agents such as vinyl chloride and pesticides (Alifieris and Trafalis 2015). Furthermore, a group of specific genetic disorders such as retinoblastoma, neurofibromatosis type 1 and 2, Li-Fraumeni syndrome, tuberous sclerosis, and Turcot syndrome may increase the risk of GBM (Ellor et al. 2014).

Clinical presentations of the tumor are highly dependent on the size and the location of the tumor. The most common reasons patients present to primary care centers are symptoms of focal weakness, speech impairment, ataxia, visual disturbances, memory loss, seizure, or increased intracranial pressure and headache (Nelson and Cha 2003; Perry et al. 2006).

Computed tomography (CT) scans or magnetic resonance imaging (MRI) are useful examination techniques for brain tumor diagnosis. In MRI, gadolinium enhancement helps doctors diagnose abnormal tissues and monitor the progress of glioblastomas. The irregular hypodense center of necrosis and heterogenous enhancement of periphery are of frequent features of GBM. Necrosis is an important diagnostic feature for a malignant brain tumor to be recognized as a case of GBM under the classification system of World Health Organization (WHO) (Blissitt 2014). Surrounding vasogenic edema, marked mass effect, intratumoral hemorrhage, and ventricular extension may also be seen on imaging (Ellor et al. 2014). Some GBMs may appear multifocal (multiple lesions at different locations), distant (lesions far from the primary focus), and diffuse or may represent microscopic infiltration, or leptomeningeal dissemination (Johnson et al. 2015).

For definitive diagnosis of GBM, examination of the neurosurgical tumor sample is done based on traditional histological, cytological, and histochemical methods and in case of no access to tumor resection, fine needle aspiration biopsy is carried out (Urbańska et al. 2014).

Fractional order calculus deals with the generalization of derivatives and integrals of arbitrary orders to non-integer orders (Podlubny 1999). In a series of papers (Agrawal et al. 2004; Hassani et al. 2022; Singh et al. 2022; Hammad et al. 2021; Wang et al. 2022; Karthikeyan et al. 2021; Rashid et al. 2022; Hajiseyedazizi et al. 2021; Rashid et al. 2022; Radmanesh and Ebadi 2020; He et al. 2022; Abdollahi et al. 2021; Jaros and Kusano 2014; Kumar et al. 2018; Odibat 2019), the authors have investigated the fractional differential equations in different branches of sciences including mathematics, physics,

bioscience, and engineering. Xu et al. (2019) analyzed Legendre-Gauss collocation method for the fractional differential equation of nonlinear distributed-order. They first proved the unique existence of the exact solution and then the high accuracy of the proposed method. Cong et al. (2020) compared solution properties of ordinary and fractional differential equations (FDEs) and proposed some distinct features and a new notion of stability for systems of fractional-order. Singla (2021) used power series expansion technique to investigate the existence of series solutions for some nonlinear systems of time fractional partial differential equations. Garrappa and Kaslik (2020) studied the initial conditions for fractional delay differential equations (FDDEs). They discussed the initialization of FDDEs on both the solution and the fractional operator and found some inconsistencies in the process of incorporating the initial function leading to the fractional derivative. Vargas (2022) presented a finite difference approach to solving a class of fractional differential equations at irregular meshes. The approach was followed on the base of moving least squares method and on the existence of a fractional Taylor polynomial for Caputo fractional derivatives. Bavi et al. (2022) developed a meshless algorithm regarding moving least squares (MLS) shape functions for solving time fractional equation of coronavirus diffusion in different mediums of soil, water, and tissue. Heydari and Atangana (2022) defined a hybrid of Chebyshev and piecewise Chebyshev cardinal functions to solve nonlinear equations of fractional reaction-advection-diffusion. Roohi et al. (2021) simulated the behavior of the generalized Couette flow of fractional Jeffrey nanofluid subjected to porous medium of fluctuating thermochemical effects based on the second kind Chebyshev polynomials. Hosseininia and Heydari (2019) proposed a meshless MLS method for the numerical solution of nonlinear equations of 2D telegraph involving Mittag-Leffler non-singular kernel in the Atangana–Baleanu–Caputo sense using variable-order time fractional derivatives. Heydari et al. (2014) proposed a novel computational approach for solving fractional biharmonic equations based on the combination of operational matrix of fractional derivatives and shifted polynomials of Chebyshev. Sabermahani et al. (2020) achieved a new operational Tau-Collocation method on the Lagrange polynomial basis to find the solution of fractional differential equations of variable order. Bhrawy et al. (2014) used generalized Laguerre orthogonal functions of fractional order to approximate a system of fractional differential equations via a new spectral method. Hussien (2019) developed a collocation operational matrix method for two common delay differential equations of fractional order on generalized Laguerre polynomial basis. Zaky (2020) provided an adaptive spectral collocation method to approximate the solution of a general nonlinear system of

fractional differential equations and non-smooth solutions of related integral equations. Zaky (2019) derived an exponentially accurate approach of Jacobi spectral-collocation for non-smooth solutions to nonlinear terminal value problems. Abo-Gabal et al. (2022) proposed Romanovski-Jacobi-Gauss-type quadrature formulae for spectral tau approximation of non-smooth solutions of time-fractional partial differential equations.

Laguerre polynomials (LPs) are widely used as basis functions to numerically solve various types of differential equations. Bhrawy et al. (2014) proposed a formula to express any of Caputo fractional order derivatives in terms of fractional order generalized Laguerre functions. In addition, a fractional order generalized tau technique was proposed for solving Caputo type fractional differential equations. Daşcıoğlu and Varol (2021) used LPs to develop an approximation method for the numerical solutions of linear fractional Fredholm–Volterra integro-differential equations. Yu et al. (2019) employed the generalized associated Laguerre functions of the first kind as basis functions to numerically solve time-fractional sub-diffusion equations in two-dimensional space on an unbounded domain. Shiralashetti and Kumbinaraiah (2020) developed a numerical algorithm to find a numerical solution for the system of differential equations based on the Laguerre wavelets exact Parseval frame. Hussien (2019) proposed a collocation method for an approximation of two common delay differential equations of fractional order with generalized LPs basis. Hajimohammadi and Parand (2021) applied a new learning approximation method of generalized Laguerre least squares support vector regression (GLLSSVR) to obtain the solution of time-fractional sub diffusion model (TFSDM) over a semi-infinite domain. Their new method was a combination of collocation/Galerkin method and a kernel of LSSVR method. Chi and Jiang (2021) proposed Laguerre-Legendre spectral method to approximate time direction for the flow of two-dimensional generalized Oldroyd-B model in semi-infinite intervals. Shahni and Singh (2022) proposed three computational algorithms based on Taylor-wavelet, Gegenbauer-wavelet, and Laguerre-wavelet collocation methods to solve the integral form of Emden-Fowler equations with a kernel of Green's functions. Chen et al. (2021) used a novel Laguerre neural network with three layers of neurons for solving Black–Scholes equations and proved its high accuracy and superiority over other existing algorithms. Zhang and Miao (2017) applied weighted LPs to an unconditionally stable scheme for solving one-dimensional telegraph equation.

This paper proposes and applies a fractional order model of glioblastoma brain tumor. The interesting feature of this work is that the LPs are extended to the generalized Laguerre polynomials (GLPs) as a new class of basis function which enables easy approximation of the unknown function and its derivatives. The solution methodology is

based on the operational matrices of GLPs and the Lagrange multipliers which reduces solving the model into a nonlinear system of algebraic equations. The proposed model is thus simple and easy to implement for the problem under study whose optimal solution is obtained by solving a system of nonlinear equations. The convergence analysis is also presented for the study model. Furthermore, some test examples are given to verify the validity as well as the applicability of the model.

The distinction between other spectral methods and our proposed approach must be highlighted from the numerical point of view. The error between the exact and numerical solutions must be minimized from an ideal point of view. Accordingly, coefficients must be determined in line with the underlying idea of spectral methods such as Chebyshev, Jacobi, Legendre, and Lagrange polynomials, expressing the solution of a differential equation as a sum of basis functions. There are three common techniques of tau, Galerkin, and collocation used to determine the coefficients. Here, the residual function and the 2-norm of the residual are utilized to transform the study problem into an optimization one and to obtain unknown parameters optimally. Therefore, optimality conditions are found in the form of a nonlinear system of algebraic equations with unknown coefficients. On the other hand, any arbitrary smooth function can be spectrally approximated by singular Sturm–Liouville eigenfunctions such as Chebyshev, Legendre, Jacobi, Lagrange, Hermite, or Laguerre polynomials. In other words, the truncation error tends to zero in a faster way than the potential number of basis functions approaches infinity in the approximation. In conclusion, these basis functions are not most optimally suited to non-analytic function approximation. For this purpose, the use of GLPs is much more efficient.

This work is prepared as follows. In Sect. 2, formulation of fractional order glioblastoma tumor (FGT) and some definitions of fractional calculus are given in the sense of Caputo. In Sect. 3, GLPs are constructed and used to provide operational matrices of derivative, function approximation, and convergence analysis. In Sect. 4, description and analysis of the presented method are made. In Sect. 5, application of the GLPs algorithm is investigated for three examples. In Sect. 6, some concluding remarks are finally drawn.

2 Fractional Order Glioblastoma Tumor in the Caputo Derivative Sense

Glioblastoma multiforme (GBM), also known as a grade IV astrocytoma, starts in brain cells called glial cells. The grading system of gliomas from I to IV indicates the likely progress and growth of brain tumor. Grade IV tumor as the most aggressive type grows rapidly. The tumor may

display central necrosis and the tumors cells divide actively. There are more areas of dead tissue and abnormal blood vessel growth. Many researchers have simulated the original two-dimensional model of brain tumor to predict the equation of tumor growth (Cruywagen et al. 1995; Tracqui et al. 1995; Woodward et al. 1996). They have described the effect of therapy on the spatiotemporal growth of tumor by using models that can be read as,

Rate of change of tumor cell density
= Diffusion of tumor cells + Growth of tumor cells

in mathematical terms,

$$\begin{aligned} \frac{\partial U(x, t)}{\partial t} &= \mathcal{D}\nabla^2 U(x, t) + \varrho U(x, t) \\ &= \mathcal{D} \frac{1}{x^2} \frac{\partial}{\partial x} \left(x^2 \frac{\partial U(x, t)}{\partial x} \right) + \varrho U(x, t). \end{aligned} \tag{2.1}$$

Here, $U(x, t)$ shows the concentration of tumor cells at location x at time t ∇^2 indicates the Laplacian operator, and \mathcal{D} represents diffusion coefficient as a measure of the spread of invading glioblastoma cells per day in terms of cm^2 . The reproduction rate of glioblastoma cells is expressed by ϱ as a decimal fraction per day. Some authors have added a term of killing rate to investigate the effects of chemotherapy as,

Rate of change of tumor cell density
= Diffusion of tumor cells + Growth of tumor cells
– Killing rate of tumor cells,

Mathematically,

$$\begin{aligned} \frac{\partial U(x, t)}{\partial t} &= \mathcal{D} \frac{1}{x^2} \frac{\partial}{\partial x} \left(x^2 \frac{\partial U(x, t)}{\partial x} \right) \\ &+ \varrho U(x, t) - \kappa_t U(x, t). \end{aligned} \tag{2.2}$$

where κ_t is the killing rate of of tumor cells. Equation (2.2) can be rewritten as

$$\begin{aligned} \frac{\partial U(x, t)}{\partial t} &= \mathcal{D} \left(\frac{\partial^2 U(x, t)}{\partial x^2} + \frac{2}{x} \frac{\partial U(x, t)}{\partial x} \right) \\ &+ (\varrho - \kappa_t) U(x, t). \end{aligned} \tag{2.3}$$

Assume $\tau = 2\mathcal{D}t$ and $V(x, \tau) = xU(x, t)$, then

$$\partial\tau = 2\mathcal{D}\partial t \Rightarrow \frac{\partial t}{\partial\tau} = \frac{1}{2\mathcal{D}}. \tag{2.4}$$

From (2.4), we get

$$\begin{aligned} \frac{\partial V(x, \tau)}{\partial\tau} &= x \frac{\partial U(x, t)}{\partial\tau} \\ &= x \frac{\partial U(x, t)}{2\mathcal{D}\partial t} = \frac{x}{2\mathcal{D}} \frac{\partial U(x, t)}{\partial t}, \end{aligned} \tag{2.5}$$

and

$$\begin{aligned} \frac{\partial V(x, \tau)}{\partial x} &= x \frac{\partial U(x, t)}{\partial x} + U(x, t), \\ \frac{\partial^2 V(x, \tau)}{\partial x^2} &= x \frac{\partial^2 U(x, t)}{\partial x^2} + 2 \frac{\partial U(x, t)}{\partial x}. \end{aligned} \tag{2.6}$$

In view of (2.5) and (2.6), we can write

$$\begin{aligned} \frac{\partial U(x, t)}{\partial t} &= \frac{2\mathcal{D}}{x} \frac{\partial V(x, \tau)}{\partial\tau}, \\ \frac{\partial U(x, t)}{\partial x} &= \frac{1}{x} \left(\frac{\partial V(x, \tau)}{\partial x} - U(x, t) \right), \\ \frac{\partial^2 U(x, t)}{\partial x^2} &= \frac{1}{x} \left(\frac{\partial^2 V(x, \tau)}{\partial x^2} - 2 \frac{\partial U(x, t)}{\partial x} \right). \end{aligned} \tag{2.7}$$

Using this, the Eq. (2.2) becomes

$$\frac{\partial V(x, \tau)}{\partial\tau} = \frac{1}{2} \frac{\partial^2 V(x, \tau)}{\partial x^2} + \frac{\varrho - \kappa_t}{\mathcal{D}} V(x, \tau). \tag{2.8}$$

Now, suppose $W(x, \tau) = \frac{\varrho - \kappa_t}{\mathcal{D}} V(x, \tau)$ and $V(x, \tau_0)$ is initial growth-profile, then

$$\begin{aligned} \frac{\partial V(x, \tau)}{\partial\tau} &= \frac{1}{2} \frac{\partial^2 V(x, \tau)}{\partial x^2} + W(x, \tau), \\ V(x, \tau_0) &= v(x). \end{aligned} \tag{2.9}$$

Memory properties have been broadly applied to many complex phenomena in applied sciences. The use of fractional derivatives, for their extra degree of freedom, compared to the use of integer ones may achieve better results. Concerning intrinsic properties of nonlocal operators, fractional differential equations are more helpful in explaining phenomena or processes related to hereditary or memory properties in areas of biology, chemistry, economy, and physics. Readers can refer to Lorenzo and Hartley (2000); Sun et al. (2011).

$$\begin{aligned} {}^C_0 D_\tau^\theta V(x, \tau) &= \frac{1}{2} \frac{\partial^2 V(x, \tau)}{\partial x^2} + W(x, \tau), \\ V(x, \tau_0) &= v(x). \end{aligned} \tag{2.10}$$

where ${}^C_0 D_\tau^\theta$ refers to the fractional derivative operator of order θ in the Caputo sense with $0 < \theta \leq 1$.

Definition 1 The fractional Caputo derivative of order $\theta \in (m - 1, m]$, $m \in \mathbb{N}$ of $V(x, \tau)$ with respect to τ is represented by Hassani et al. (2019, 2020)

$$\begin{aligned} {}^C_0 D_\tau^\theta V(x, \tau) &= \\ &\begin{cases} \frac{1}{\Gamma(m - \theta)} \int_0^\tau (\tau - \xi)^{m-\theta-1} \frac{\partial^m V(x, \xi)}{\partial \xi^m} d\xi, & \theta \in (m - 1, m), \\ \frac{\partial^m V(x, \tau)}{\partial \tau^m}, & \theta = m, \end{cases} \end{aligned} \tag{2.11}$$

where $\Gamma(\cdot)$ implies the gamma function.

Corollary 1 The definition 1 for $k \in \mathbb{N} \cup \{0\}$ results in

$${}^C_0D_\tau^\theta \tau^k = \begin{cases} \frac{\Gamma(k+1)}{\Gamma(k-\theta+1)} \tau^{k-\theta}, & k \geq m, \\ 0, & k < m, \end{cases} \quad (2.12)$$

where $\theta \in (m-1, m]$.

Definition 2 The two-parameter Mittag-Leffler function $E_{\alpha, \zeta}(z)$ is defined as Hassani et al. (2019, 2020)

$$E_{\alpha, \zeta}(z) = \sum_{j=0}^{\infty} \frac{z^j}{\Gamma(j\alpha + \zeta)},$$

where α and ζ are positive constants.

3 Required Tools

In this section, we first introduce GLPs and operational matrices to solve FGT, then provide function approximation and convergence analysis.

3.1 Description of the GLPs

In this subsection, the main concepts of the GLPs are introduced to make some approximation of the given function.

Definition 3 (see Aizenshtadt et al. 1966 and references therein) The Laguerre polynomials (LPs), $\mathcal{L}_n(\tau)$, are solutions to linear differential equation of second order $xy'' + (1-x)y' + ny = 0$, $n \in \mathbb{N}$.

Definition 4 (see Aizenshtadt et al. 1966 and references therein) The representation of power series for LPs, $\mathcal{L}_n(\tau)$, is provided by

$$\mathcal{L}_n(\tau) = \sum_{k=0}^n \frac{(-1)^k}{k!} \frac{(n)!}{(k!(n-k)!)} \tau^k. \quad (3.1)$$

The first LPs are given by:

$$\begin{aligned} \mathcal{L}_0(\tau) &= 1, \\ \mathcal{L}_1(\tau) &= -\tau + 1, \\ \mathcal{L}_2(\tau) &= \frac{1}{2}(\tau^2 - 4\tau + 2), \\ \mathcal{L}_3(\tau) &= \frac{1}{6}(-\tau^3 + 9\tau^2 - 18\tau + 6). \end{aligned}$$

The given function $u(\tau)$ can be approximated generally with the first $n + 1$ LPs terms as

$$u(\tau) \simeq P^T Q \Psi_n(\tau), \quad (3.2)$$

where

$$Q = \begin{pmatrix} q_{00} & q_{01} & \cdots & q_{0n} \\ q_{10} & q_{11} & \cdots & q_{1n} \\ \vdots & \vdots & \ddots & \vdots \\ q_{n0} & q_{n1} & \cdots & q_{nn} \end{pmatrix}, \quad (3.3)$$

$$P^T = [p_0 \ p_1 \ \dots \ p_n], \Psi_n(\tau) = [1 \ \tau \ \tau^2 \ \dots \ \tau^n]^T,$$

and

$$q_{ij} = \begin{cases} \frac{(-1)^j}{j!} \frac{(i)!}{(j!(i-j)!)}, & i \geq j, \\ 0, & i < j. \end{cases} \quad (3.4)$$

Definition 5 The GLPs, $\mathcal{L}_m(\tau)$, are formed with a change of variable. Accordingly, τ^i is changed to $\tau^{i+\beta_i}$, ($i + \beta_i > 0$), on the LPs and defined as

$$\mathcal{L}_m(\tau) = \sum_{k=0}^m \frac{(-1)^k}{k!} \frac{(m)!}{(k!(m-k)!)} \tau^{k+\beta_k}, \quad (3.5)$$

where β_k indicate control parameters. If $\beta_k = 0$, then GLPs fully coincide with classical LPs.

The expansion of $v(\tau)$ functions in terms of GLPs can be shown in the form of matrices

$$v(\tau) = R^T S \Phi_m(\tau), \quad (3.6)$$

where

$$S = \begin{pmatrix} s_{0,0} & s_{0,1} & s_{0,2} & \cdots & s_{0,m} \\ s_{1,0} & s_{1,1} & s_{1,2} & \cdots & s_{1,m} \\ s_{2,0} & s_{2,1} & s_{2,2} & \cdots & s_{2,m} \\ \vdots & \vdots & \vdots & \dots & \vdots \\ s_{m,0} & s_{m,1} & s_{m,2} & \cdots & s_{m,m} \end{pmatrix}, \quad R^T = [r_0 \ r_1 \ \dots \ r_m], \Phi_m(t) = [1 \ \tau^{1+\beta_1} \ \tau^{2+\beta_2} \ \dots \ \tau^{m+\beta_m}]^T, \quad (3.7)$$

and

$$s_{ij} = \begin{cases} \frac{(-1)^j}{j!} \frac{(i)!}{(j!(i-j)!)}, & i \geq j, \\ 0, & i < j, \end{cases} \quad (3.8)$$

where β_k , $k = 1, 2, \dots, m$, are control parameters.

The following matrices can explain the expansion of given functions $V(x, \tau)$ by means of GLPs:

$$V(x, \tau) \simeq \Phi_{m_1}(x)^T \mathcal{A} \Psi_{m_2}(\tau), \quad (3.9)$$

where $\mathcal{A} = [a_{ij}]$ are $(m_1 + 1) \times (m_2 + 1)$ unknown matrices of free coefficients, that must be computed. The vectors $\Phi_{m_1}(x)$ and $\Psi_{m_2}(\tau)$ are defined as:

$$\Phi_{m_1}(x) = \mathcal{C} \mathcal{F}_{m_1}(x), \Psi_{m_2}(\tau) = \mathcal{D} \mathcal{G}_{m_2}(\tau), \tag{3.10}$$

where

$$\mathcal{F}_{m_1}(x) = [f_0(x) \ f_1(x) \ \dots \ f_{m_1}(x)]^T, \tag{3.11}$$

$$\mathcal{G}_{m_2}(\tau) = [g_0(\tau) \ g_1(\tau) \ \dots \ g_{m_2}(\tau)]^T,$$

$$\mathcal{A} = \begin{pmatrix} a_{0,0} & a_{0,1} & \dots & a_{0,m_2} \\ a_{1,0} & a_{1,1} & \dots & a_{1,m_2} \\ \vdots & \vdots & \dots & \vdots \\ a_{m_1,0} & a_{m_1,1} & \dots & a_{m_1,m_2} \end{pmatrix}, \tag{3.12}$$

$$\mathcal{C} = \begin{pmatrix} 1 & 0 & 0 & \dots & 0 \\ 0 & 1 & 0 & \dots & 0 \\ c_{2,0} & c_{2,1} & c_{2,2} & \dots & c_{2,m_1} \\ \vdots & \vdots & \vdots & \dots & \vdots \\ c_{m_1,0} & c_{m_1,1} & c_{m_1,2} & \dots & c_{m_1,m_1} \end{pmatrix}, \tag{3.13}$$

$$\mathcal{D} = \begin{pmatrix} 1 & 0 & 0 & \dots & 0 \\ d_{1,0} & d_{1,1} & d_{1,2} & \dots & d_{1,m_2} \\ d_{2,0} & d_{2,1} & d_{2,2} & \dots & d_{2,m_2} \\ \vdots & \vdots & \vdots & \dots & \vdots \\ d_{m_2,0} & d_{m_2,1} & d_{m_2,2} & \dots & d_{m_2,m_2} \end{pmatrix},$$

$$c_{ij} = \begin{cases} \frac{(-1)^j}{j!} \frac{(i)!}{(j!)(i-j)!}, & i \geq j, \\ 0, & i < j, \end{cases} \quad \begin{matrix} i = 2, 3, \dots, m_1, \\ j = 0, 1, \dots, m_1, \end{matrix} \tag{3.14}$$

$$d_{ij} = \begin{cases} \frac{(-1)^j}{j!} \frac{(i)!}{(j!)(i-j)!}, & i \geq j, \\ 0, & i < j, \end{cases} \quad \begin{matrix} i = 1, 2, \dots, m_2, \\ j = 0, 1, \dots, m_2, \end{matrix} \tag{3.15}$$

$$f_i(x) = \begin{cases} x^i, & i = 0, 1, \\ x^{i+k_i}, & i = 2, 3, \dots, m_1, \end{cases} \tag{3.16}$$

$$g_j(\tau) = \begin{cases} 1, & j = 0, \\ \tau^{j+s_j}, & j = 1, 2, \dots, m_2, \end{cases}$$

where k_i and s_j are control parameters.

3.2 Operational Matrix

The fractional derivative of order $0 < \theta \leq 1$, of $\mathcal{G}_{m_2}(\tau)$ can be written as

$${}^C D_\tau^\theta \mathcal{G}_{m_2}(\tau) = \mathcal{D}_\tau^{(\theta)} \mathcal{G}_{m_2}(\tau), \tag{3.17}$$

where $\mathcal{D}_\tau^{(\theta)}$ denotes the $(m_2 + 1) \times (m_2 + 1)$ operational matrix of fractional derivative, defined by:

$$\mathcal{D}_\tau^{(\theta)} = \begin{pmatrix} 0 & 0 & 0 & 0 & \dots & 0 \\ 0 & \frac{\Gamma(2+s_1)}{\Gamma(2-\theta+s_1)} & 0 & 0 & \dots & 0 \\ 0 & 0 & \frac{\Gamma(3+s_2)}{\Gamma(3-\theta+s_2)} & 0 & \dots & 0 \\ \vdots & \vdots & \vdots & \vdots & \ddots & \vdots \\ 0 & 0 & 0 & 0 & \dots & \frac{\Gamma(m_2+1+s_{m_2})}{\Gamma(m_2+1-\theta+s_{m_2})} \end{pmatrix}, \tag{3.18}$$

The second order derivatives of $\mathcal{F}_{m_1}(x)$ is given by:

$$\frac{d^2 \mathcal{F}_{m_1}(x)}{dx^2} = \mathcal{D}_x^{(2)} \mathcal{F}_{m_1}(x), \tag{3.19}$$

where $\mathcal{D}_x^{(2)}$ denotes $(m_1 + 1) \times (m_1 + 1)$ operational matrix of derivative:

$$\mathcal{D}_x^{(2)} = \begin{pmatrix} 0 & 0 & 0 & \dots & 0 \\ 0 & 0 & 0 & \dots & 0 \\ 0 & 0 & \frac{(2+k_2)(1+k_2)}{x^2} & \dots & 0 \\ \vdots & \vdots & \vdots & \ddots & \vdots \\ 0 & 0 & 0 & \dots & \frac{(m_1+k_{m_1})(m_1-1+k_{m_1})}{x^2} \end{pmatrix}, \tag{3.20}$$

where k_i , ($i = 2, 3, \dots, m_1$) and s_j , ($j = 1, 2, \dots, m_2$) are control parameters, $\Gamma(\cdot)$ is the gamma function, m_1 and m_2 are numbers of basis functions and θ is the fractional order.

3.3 Function Approximation

Let $\mathbb{X} = L^2[0, 1] \times [0, 1]$ and $\mathbb{Y} = \langle x^{k_i} \tau^{s_j}; 0 \leq i \leq m_1, 0 \leq j \leq m_2 \rangle$. Then, \mathbb{Y} suggests a subspace of finite dimensional vector space of \mathbb{X} ($\dim \mathbb{Y} \leq (m_1 + 1)(m_2 + 1) < \infty$) with each $\tilde{V} = \tilde{V}(x, \tau) \in X$ converging to a unique best approximation $V_0 = V_0(x, \tau) \in \mathbb{Y}$, given by:

$$\forall \hat{V} \in \mathbb{Y}, \quad \| \tilde{V} - V_0 \|_2 \leq \| \tilde{V} - \hat{V} \|_2.$$

More details are evident in Theorem 6.1-1 of Kreyszig (1987). The $V_0 \in \mathbb{Y}$ and \mathbb{Y} finite dimensional vector subspace of \mathbb{X} provide us with unique coefficients $a_{ij} \in \mathbb{R}$. From an elementary argument in linear algebra, we obtain coefficients such that $V_0(x, \tau)$ dependent variable can be expanded in terms of polynomials of

$$V_0(x, \tau) \simeq \Phi_{m_1}(x)^T \mathcal{A} \Psi_{m_2}(\tau),$$

where $\Phi_{m_1}(x)^T$ and $\Psi_{m_2}(\tau)$ are defined in Eq. (3.10).

3.4 Convergence Analysis

Theorem 1 Suppose $f : Q \rightarrow \mathbb{R}$ is $(m_1 + m_2 + 1)$ times continuously differentiable, say for $i = 1, 2, \dots, m_1 + m_2 + 1$, $\left| \frac{\partial^{m_1+m_2+1}}{\partial t^{m_1+m_2+1}} f(x, t) \right| \leq M_2$. Let $Y = \langle x^{k_i} \tau^{s_j} : 0 \leq i \leq m_1, 0 \leq j \leq m_2, k_i, s_j \geq 0 \rangle$, where Y is a linear subspace with finite dimension of $L^2(Q)$. If $\Phi_{m_1}^T$ is a unique best approximation of f out of Y where $\Phi_{m_1}(x)$ and $\Psi_{m_2}(\tau)$ are given in (3.9) and $\mathcal{A} = [a_{ij}] : i = 1, 2, \dots, m_1, j = 1, 2, \dots, m_2$ is the coefficient matrix, then the following holds:

$$\begin{aligned} & \| \tilde{V}(x, \tau) - \Phi_{m_1}(x) \mathcal{A} \Psi_{m_2}(\tau) \|_2 \\ & \leq \frac{\Gamma(k+1) M_2 \sqrt{M_3(m_1+m_2+2)}}{l!(m_1+m_2+1-l)!}, \end{aligned} \tag{3.21}$$

where $M_3 = \max \left\{ \frac{\Gamma(2i+k+1)\Gamma(2m_1+2m_2+3-2i+s)}{\Gamma(k+s+2i+2)\Gamma(k+s+2m_1+2m_2+4-2i)} : i = 1, 2, \dots, m_1+m_2+1 \right\}$.

Proof Given Maclaurin’s expression for $\tilde{V}(x, \tau)$

$$\begin{aligned} \tilde{V}(x, \tau) &= p(x, \tau) \\ &+ \frac{1}{(m_1+m_2+1)!} \left(x \frac{\partial}{\partial x} + \tau \frac{\partial}{\partial \tau} \right)^{m_1+m_2+1} \tilde{V}(\xi_0 x, \xi_0 \tau), \quad \xi \in (0, 1) \end{aligned} \tag{3.22}$$

where $p(x, \tau) = \sum_{r=0}^{m_1+m_2} \frac{1}{r!} \left(x \frac{\partial}{\partial x} + \tau \frac{\partial}{\partial \tau} \right)^r \tilde{V}(0, 0)$. This implies that

$$\begin{aligned} & | \tilde{V}(x, \tau) - p(x, \tau) | \\ &= \left| \frac{1}{(m_1+m_2+1)!} \left(x \frac{\partial}{\partial x} + \tau \frac{\partial}{\partial \tau} \right)^{m_1+m_2+1} \tilde{V}(\xi_0 x, \xi_0 \tau) \right|, \quad \xi \in (0, 1) \end{aligned} \tag{3.23}$$

On the other hand, since $\Phi_{m_1}(x) \mathcal{A} \Psi_{m_2}(\tau)$ is the best approximation of $\tilde{V}(x, \tau)$ we obtain

$$\| \tilde{V}(x, \tau) - \Phi_{m_1}(x) \mathcal{A} \Psi_{m_2}(\tau) \|_2 \leq \| \tilde{V}(x, \tau) - p(x, \tau) \|_2.$$

Now, in view of definition of L^2 -norm, we get

$$\begin{aligned} & \| \tilde{V}(x, \tau) - \Phi_{m_1}(x) \mathcal{A} \Psi_{m_2}(\tau) \|_2^2 \\ &= \int_0^1 \int_0^1 \left[\frac{1}{(m_1+m_2+1)!} \left(x \frac{\partial}{\partial x} + \tau \frac{\partial}{\partial \tau} \right)^{m_1+m_2+1} \right]^2 dx d\tau \\ &= \int_0^1 \int_0^1 \left[\frac{1}{(m_1+m_2+1)!} \sum_{i=0}^{m_1+m_2+1} \binom{m_1+m_2+1}{i} x^{m_1+m_2+1-i} \tau^i \right. \\ & \quad \left. \frac{\partial^{m_1+m_2+1}}{\partial x^{m_1+m_2+1} \partial \tau^i} \right]^2 dx d\tau \\ &\leq \frac{M_2^2}{(m_1+m_2+1)!} \int_0^1 \int_0^1 \left[\sum_{i=0}^{m_1+m_2+1} \binom{m_1+m_2+1}{r} x^{m_1+m_2+1-i} \tau^i \right]^2 dx d\tau, \end{aligned}$$

where $\binom{m_1+m_2+1}{r} = \max \left\{ \binom{m_1+m_2+1}{i} : i = 1, 2, \dots, m_1+m_2+1 \right\}$. This implies that

$$\begin{aligned} & \| \tilde{V}(x, \tau) - p \|_2^2 \\ &\leq \frac{M_2^2}{r!^2 (m_1+m_2+1)!^2} \int_0^1 \int_0^1 \left[\sum_{i=0}^{m_1+m_2+1} x^{m_1+m_2+1-i} \tau^i \right]^2 dx d\tau \\ &\leq \frac{M_2^2}{r!^2 (m_1+m_2+1)!^2} \\ & \quad \sum_{i=0}^{m_1+m_2+1} \frac{\Gamma(2i+k+1)\Gamma(2m_1+2m_2+3-2i+s)}{\Gamma(k+s+2i+2)\Gamma(k+s+2m_1+2m_2+4-2i)} \\ &\leq \frac{\Gamma(k+1)^2 M_3 (m_1+m_2+2) M_2^2}{l^2 (m_1+m_2+1-l)!^2}, \end{aligned}$$

which is the desired result. \square

4 Solution Procedure

In this section, based on the GLPs, an optimization method is presented to solve the study problem (2.10). $V(x, \tau)$ dependent variable can be expanded in terms of GLPs as

$$V(x, \tau) \simeq \Phi_{m_1}(x)^T \mathcal{A} \Psi_{m_2}(\tau) = (\mathcal{C} \mathcal{F}_{m_1}(x))^T \mathcal{A} (\mathcal{D} \mathcal{G}_{m_2}(\tau)), \tag{4.1}$$

where $\mathcal{A} = [a_{ij}]$ is undetermined matrix, and $\mathcal{F}_{m_1}(x)$ and $\mathcal{G}_{m_2}(\tau)$ are in obedience to Eq. (3.11). From Eqs. (3.17) and (3.19), we have

$$\begin{aligned} {}_0^C D_\tau^\theta V(x, \tau) &\simeq (\mathcal{C} \mathcal{F}_{m_1}(x))^T \mathcal{A} \left(\mathcal{D} D_\tau^{(\theta)} \mathcal{G}_{m_2}(\tau) \right), \\ V_{xx}(x, \tau) &\simeq \left(\mathcal{C} D_x^{(2)} \mathcal{F}_{m_1}(x) \right)^T \mathcal{A} (\mathcal{D} \mathcal{G}_{m_2}(\tau)). \end{aligned} \tag{4.2}$$

Replacing Eqs. (4.1) and (4.2) into the initial conditions yield

$$\Lambda(x) \triangleq (\mathcal{C} \mathcal{F}_{m_1}(x))^T \mathcal{A} (\mathcal{D} \mathcal{G}_{m_2}(\tau_0)). \tag{4.3}$$

Substituting Eqs. (4.1) and (4.2) into Eq. (2.10), we get

$$\begin{aligned} \mathcal{R}(x, \tau, \mathcal{A}, \mathcal{K}, \mathcal{S}) &\triangleq (\mathcal{C} \mathcal{F}_{m_1}(x))^T \mathcal{A} \left(\mathcal{D} D_\tau^{(\theta)} \mathcal{G}_{m_2}(\tau) \right) \\ &\quad - \frac{1}{2} \left(\mathcal{C} D_x^{(2)} \mathcal{F}_{m_1}(x) \right)^T \mathcal{A} (\mathcal{D} \mathcal{G}_{m_2}(\tau)) - W(x, \tau). \end{aligned} \tag{4.4}$$

Here \mathcal{A} stands for unknown free coefficients and \mathcal{K} and \mathcal{S} stand for unknown control vectors, respectively, for $\mathcal{F}_{m_1}(x)$ and $\mathcal{G}_{m_2}(\tau)$, defined as

$$\mathcal{K} = [k_2 \ k_3 \ \dots \ k_{m_1}], \quad \mathcal{S} = [s_1 \ s_2 \ \dots \ s_{m_2}]. \tag{4.5}$$

The two-norm of the residual vectors can be given by

$$\mathcal{M}(\mathcal{A}, \mathcal{K}, \mathcal{S}) = \int_0^{l_2} \int_0^{l_1} \mathcal{R}^2(x, \tau, \mathcal{A}, \mathcal{K}, \mathcal{S}) dx d\tau. \tag{4.6}$$

To find the optimal solution, control parameters \mathcal{K} and \mathcal{S}

and undetermined matrix \mathcal{A} must be evaluated. The optimization problem is therefore considered as

$$\min \mathcal{M}(\mathcal{A}, \mathcal{K}, \mathcal{S}), \tag{4.7}$$

subject to

$$\Lambda \left(\frac{i}{m_1} \right) = 0, i = 0, 1, \dots, m_1. \tag{4.8}$$

To solve the minimization problem, the Lagrange multipliers method is used.

$$\mathcal{J}^*[\mathcal{A}, \mathcal{K}, \mathcal{S}; \lambda] = \mathcal{M}(\mathcal{A}, \mathcal{K}, \mathcal{S}) + \lambda \Lambda, \tag{4.9}$$

where the vector λ corresponds to unknown Lagrange multipliers and Λ express a known column vector with entries of equality constraints in accordance to Eq. (4.8). The following nonlinear system of algebraic equations presents necessary conditions for local extremum.

$$\frac{\partial \mathcal{J}^*}{\partial \mathcal{A}} = 0, \frac{\partial \mathcal{J}^*}{\partial \mathcal{K}} = 0, \frac{\partial \mathcal{J}^*}{\partial \mathcal{S}} = 0, \frac{\partial \mathcal{J}^*}{\partial \lambda} = 0. \tag{4.10}$$

This nonlinear system of algebraic equations can be solved using software packages of MAPLE or MATLAB. The approximate solutions of the problem can be determined using control parameters and unknown free coefficients from Eq. (4.1). In the following, a brief description of the algorithm is made.

$$\begin{aligned} |e_1(x_i, \tau_i)| &= |(\mathcal{C} \mathcal{F}_{m_1}(x_i))^T \mathcal{A} (\mathcal{D} \mathcal{G}_{m_2}(\tau_i)) - V(x_i, \tau_i)|, \\ (x_i, \tau_i) &\in [0, l_1] \times [0, l_2], \\ CO &= \frac{|\log(AE_2)|}{|\log(AE_1)|}, \end{aligned}$$

where AE_1 and AE_2 , respectively, are the first and the second AE values.

Example 1 Consider the following FGT:

$$\begin{cases} {}_0^C D_\tau^\theta V(x, \tau) = \frac{1}{2} \frac{\partial^2 V(x, \tau)}{\partial x^2} \\ + \left(\frac{\Gamma\left(\frac{8}{3}\right) \tau^{-\theta}}{\Gamma\left(\frac{8}{3} - \theta\right)} - \frac{35}{8} x^{-2} \right) V(x, \tau), (x, \tau) \in [0, 1] \times [0, 1], \\ V(x, 0) = 0. \end{cases} \tag{5.1}$$

The exact solution is given by

$$V(x, \tau) = x^{\frac{7}{2}} \tau^{\frac{5}{3}}. \tag{5.2}$$

The proposed scheme is implemented to obtain the optimal solution when $m_1 = 3$, $m_2 = 1$ and $\theta = 0.80$. The obtained solution is expanded as

Algorithm (The proposed method)

Input: $m_1, m_2; \tau_0; 0 < \theta \leq 1$.

- * Define the basis functions $f_i(x)$ and $g_j(\tau)$ by (3.15).
- * Construct:
 - . the vector $\mathcal{F}_{m_1}(x)$ and $\mathcal{G}_{m_2}(\tau)$ using Eq. (3.11).
 - . the unknown matrix $\mathcal{A} = [a_{ij}]_{(m_1+1) \times (m_2+1)}$.
- * Compute:
 - . The operational matrices $\mathcal{D}_\tau^{(\theta)}$ and $\mathcal{D}_x^{(2)}$ using Eqs. (3.17) and (3.19).
 - . The residual functions $\mathcal{R}(x, \tau, \mathcal{A}, \mathcal{K}, \mathcal{S})$ using Eq. (4.4).
 - . The two-norm of the residual functions $\mathcal{M}(\mathcal{A}, \mathcal{K}, \mathcal{S})$ using Eq. (4.6).
 - . The object function $\mathcal{M}(\mathcal{A}, \mathcal{K}, \mathcal{S})$ using Eq. (4.7).
- * Minimize the objective function $\mathcal{J}^*[\mathcal{A}, \mathcal{K}, \mathcal{S}; \lambda]$ subject to the constraints (4.9).
- * Solve the nonlinear system of algebraic equations including Eq. (4.10).

Output: The optimal solution is: $V(x, \tau) \simeq \Phi_{m_1}(x)^T \mathcal{A} \Psi_{m_2}(\tau) = (\mathcal{C} \mathcal{F}_{m_1}(x))^T \mathcal{A} (\mathcal{D} \mathcal{G}_{m_2}(\tau))$.

5 Numerical Experiments

Now, the proposed scheme is applied for the solution of FGT to assess the method effectiveness. The results are then examined through calculation of both absolute error (AE) and convergence order (CO) as follows:

$$V(x, \tau) \simeq \Phi_3(x)^T \mathcal{A} \Psi_1(\tau) = (\mathcal{C} \mathcal{F}_3(x))^T \mathcal{A} (\mathcal{D} \mathcal{G}_1(\tau)),$$

where

$$\begin{aligned} \mathcal{F}_3(x) &\triangleq [1 \ x \ x^{2+k_2} \ x^{3+k_3}]^T, \\ \mathcal{G}_1(\tau) &\triangleq [1 \ \tau^{1+s_1}]^T, \end{aligned}$$

and k_2, k_3 and s_2 are control parameters. Moreover, the

matrix of unknown coefficients \mathcal{A} , and matrices of Laguerre coefficients \mathcal{C} and \mathcal{D} are given by

$$\mathcal{A} = \begin{pmatrix} a_{00} & a_{01} \\ a_{10} & a_{11} \\ a_{20} & a_{21} \\ a_{30} & a_{31} \end{pmatrix},$$

$$\mathcal{C} = \begin{pmatrix} 1 & 0 & 0 & 0 \\ 1 & -1 & 0 & 0 \\ 1 & -2 & \frac{1}{2} & 0 \\ 1 & -3 & \frac{3}{2} & \frac{-1}{6} \end{pmatrix},$$

$$\mathcal{D} = \begin{pmatrix} 1 & 0 \\ 1 & -1 \end{pmatrix}.$$

Control parameters and free coefficients are hence obtained with $m_1 = 3, m_2 = 1$ and $\theta = 0.80$ as follows

$$k_2 = 1.500124, \quad k_3 = 0.500788,$$

$$s_1 = 0.666666, \quad a_{00} = 1.248848, \quad a_{01} = -1.248848,$$

$$a_{10} = -1.370970,$$

$$a_{11} = 1.370970, \quad a_{20} = -1.004605,$$

$$a_{21} = 1.004605, \quad a_{30} = 1.126727, \quad a_{31} = -1.126726.$$

The plots of the optimal solution and AE with $m_1 = 3, m_2 = 1$ and $\theta = 0.80$ are shown in Fig. 1. The GLPs method values of AE and CO are listed in Table 1 for $m_1 = 3, m_2 = 1$ and different values of θ at various points (x, τ) . The GLPs method solves the problem with $m_1 = 3, m_2 = 3$ and $\theta = \{0.34, 0.95\}$. The AE obtained by the GLPs method with $m_1 = 3, m_2 = 3, \theta = 0.34$ (left side) and $\theta = 0.95$ (right side) are illustrated in Fig. 2. The runtime of the proposed method is reported for different choices of m_1 and m_2 in Table 2. The observed results in Table 1 and Figs. 1 and 2 are indicative of a

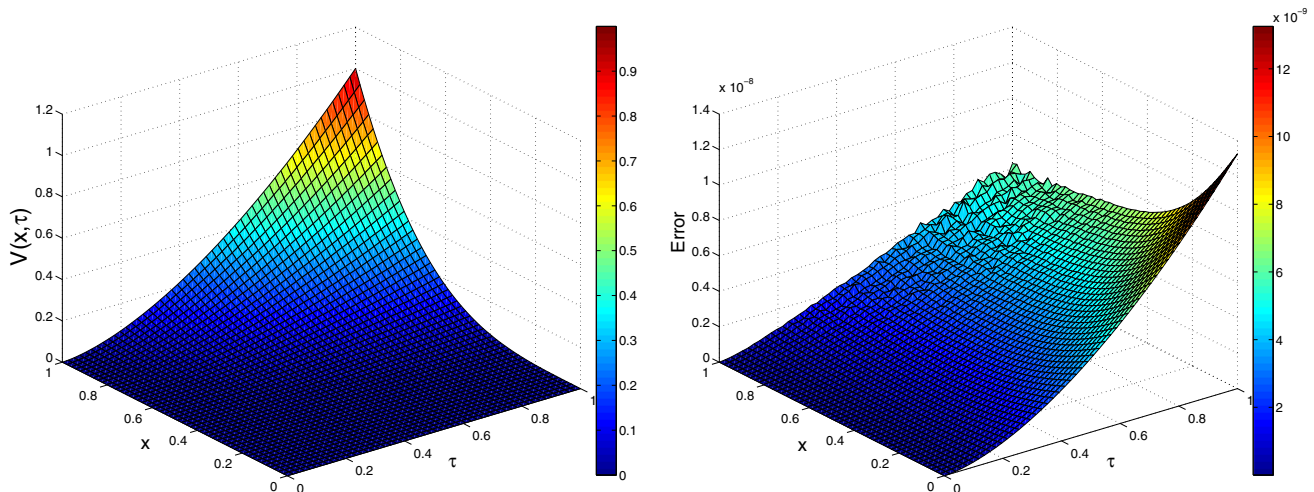


Fig. 1 The optimal solution and AE for the proposed method with $m_1 = 3, m_2 = 1$ and $\theta = 0.80$ for Example 1

Table 1 The AE and CO with $m_1 = 3, m_2 = 1$ and $\theta = \{0.70, 0.80, 0.90, 1\}$ at various points (x, τ) in Example 1

(x, τ)	$\theta = 0.70$		$\theta = 0.80$		$\theta = 0.90$		$\theta = 1$	
	AE	CO	AE	CO	AE	CO	AE	CO
(0.1, 0.1)	4.0261E-08	–	2.3800E-10	–	3.0528E-11	–	1.9781E-12	–
(0.2, 0.2)	1.0585E-07	0.9432	6.3768E-10	0.9555	7.7924E-11	0.9612	4.7226E-12	0.9677
(0.3, 0.3)	1.7645E-07	0.9681	1.1014E-09	0.9741	1.2658E-10	0.9791	6.8791E-12	0.9855
(0.4, 0.4)	2.4984E-07	0.9776	1.6389E-09	0.9807	1.7497E-10	0.9857	8.1036E-12	0.9936
(0.5, 0.5)	3.2699E-07	0.9822	2.2939E-09	0.9833	2.2414E-10	0.9889	8.1912E-12	0.9995
(0.6, 0.6)	4.0568E-07	0.9855	2.9978E-09	0.9865	2.6146E-10	0.9930	6.7029E-12	1.0078
(0.7, 0.7)	4.7946E-07	0.9886	3.7744E-09	0.9882	2.8132E-10	0.9966	2.9390E-12	1.0320
(0.8, 0.8)	5.4132E-07	0.9916	4.6782E-09	0.9889	2.8095E-10	1.0000	3.8135E-12	0.9901
(0.9, 0.9)	5.9205E-07	0.9937	5.5788E-09	0.9908	2.4275E-10	1.0066	1.3748E-11	0.9512
(1, 1)	6.5383E-07	0.9930	6.2896E-09	0.9936	1.5272E-10	1.0209	2.5673E-11	0.9750

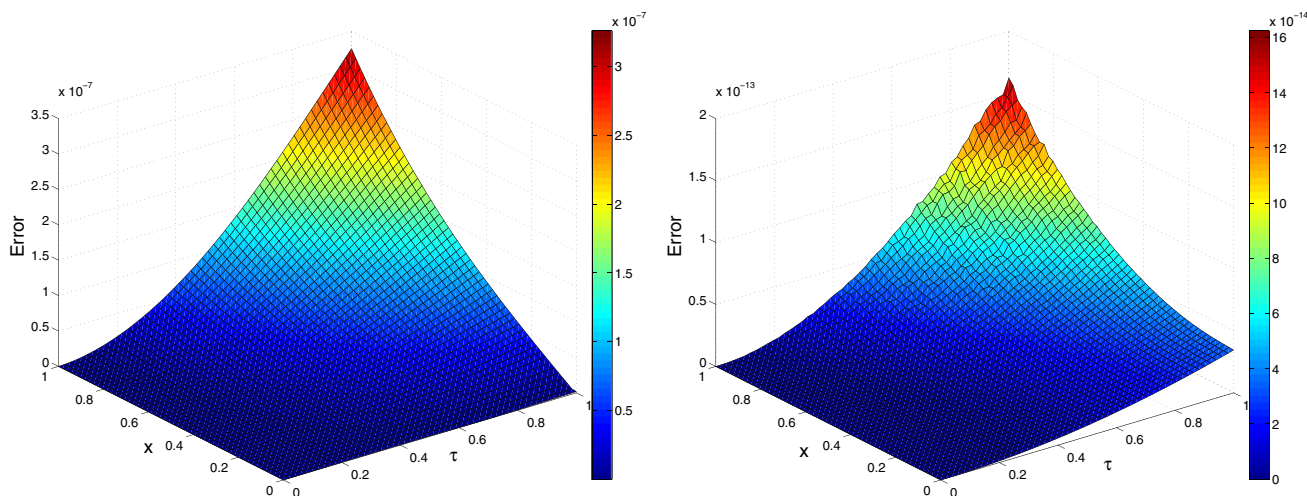


Fig. 2 The AE for the proposed method with $m_1 = 3, m_2 = 3, \theta = 0.34$ (left side) and $\theta = 0.95$ (right side) for Example 1

Table 2 The runtime (in seconds) of the proposed method with different choices of m_1 and m_2 for Example 1

case	m_1	m_2	CPU times
1	3	1	8.24
2	3	2	10.39
3	3	3	13.56
4	4	4	17.81
5	4	5	19.64

good agreement between two solutions of exact and approximate. The results also suggest that an increase in the number of basis functions can make improvement in the approximate solution.

Example 2 Consider the following FGT:

$$\begin{aligned}
 {}_0^C D_\tau^\theta V(x, \tau) &= \frac{1}{2} \frac{\partial^2 V(x, \tau)}{\partial x^2} \\
 &+ \exp(-V(x, \tau)) + \frac{1}{2} \exp(-2V(x, \tau)), (x, \tau) \in [0, 1] \times [0, 1].
 \end{aligned}
 \tag{5.3}$$

The initial condition is selected in a way that the analytical solution is $V(x, \tau) = \log(x + \tau + 2)$ when $\theta = 1$. The problem is solved by the GLPs method for parameters $m_1 = 3, m_2 = 3$ and $\theta = \{0.70, 0.80, 0.90, 1\}$, and the obtained results are shown in Table 3. Graphs of approximate solution and AE with $m_1 = 3, m_2 = 3$ and $\theta = 0.90$ are given in Fig. 3. The AE obtained by the GLPs method with $m_1 = 3, m_2 = 4, \theta = 0.76$ (left side) and $\theta = 0.87$ (right side) are represented in Fig. 4. The runtime of the proposed method with different choices of

Table 3 The AE and CO with $m_1 = 3, m_2 = 3$ and $\theta = \{0.70, 0.80, 0.90, 1\}$ at various points (x, τ) in Example 2

(x, τ)	$\theta = 0.70$		$\theta = 0.80$		$\theta = 0.90$		$\theta = 1$	
	AE	CO	AE	CO	AE	CO	AE	CO
(0.1, 0.1)	5.1716E-02	–	3.1793E-03	–	1.4399E-05	–	2.6448E-07	–
(0.2, 0.2)	6.0666E-02	0.9461	3.9706E-03	0.9613	1.8992E-05	0.9751	6.8120E-07	0.9375
(0.3, 0.3)	6.0913E-02	0.9985	4.1473E-03	0.9921	2.0616E-05	0.9924	1.1443E-06	0.9634
(0.4, 0.4)	5.7605E-02	1.0199	4.0438E-03	1.0046	2.0908E-05	0.9986	1.8270E-06	0.9657
(0.5, 0.5)	5.2831E-02	1.0303	3.8030E-03	1.0111	2.0650E-05	1.0011	2.8765E-06	0.9656
(0.6, 0.6)	4.7639E-02	1.0351	3.4952E-03	1.0151	2.0261E-05	1.0017	4.3972E-06	0.9667
(0.7, 0.7)	4.2619E-02	1.0365	3.1569E-03	1.0179	1.9966E-05	1.0013	6.4471E-06	0.9689
(0.8, 0.8)	3.8157E-02	1.0350	2.8076E-03	1.0203	1.9872E-05	1.0004	9.0425E-06	0.9716
(0.9, 0.9)	3.4573E-02	1.0302	2.4613E-03	1.0224	2.0029E-05	0.9992	1.2170E-05	0.9744
(1, 1)	3.2221E-02	1.0209	2.1344E-03	1.0237	2.0468E-05	0.9979	1.5809E-05	0.9768

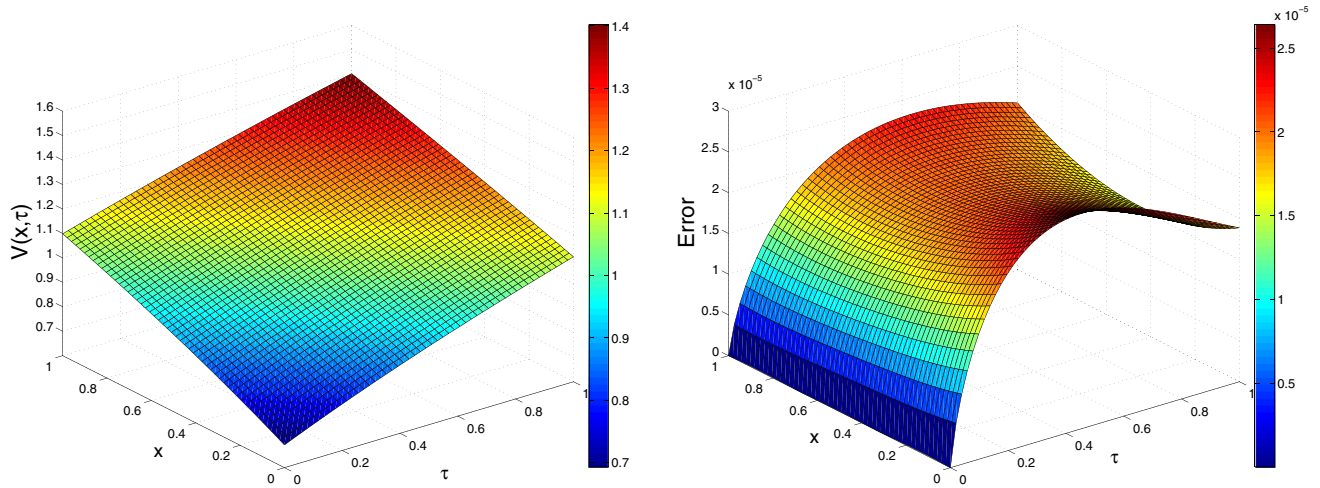


Fig. 3 The optimal solution and AE for the proposed method with $m_1 = 3, m_2 = 3$ and $\theta = 0.90$ for Example 2

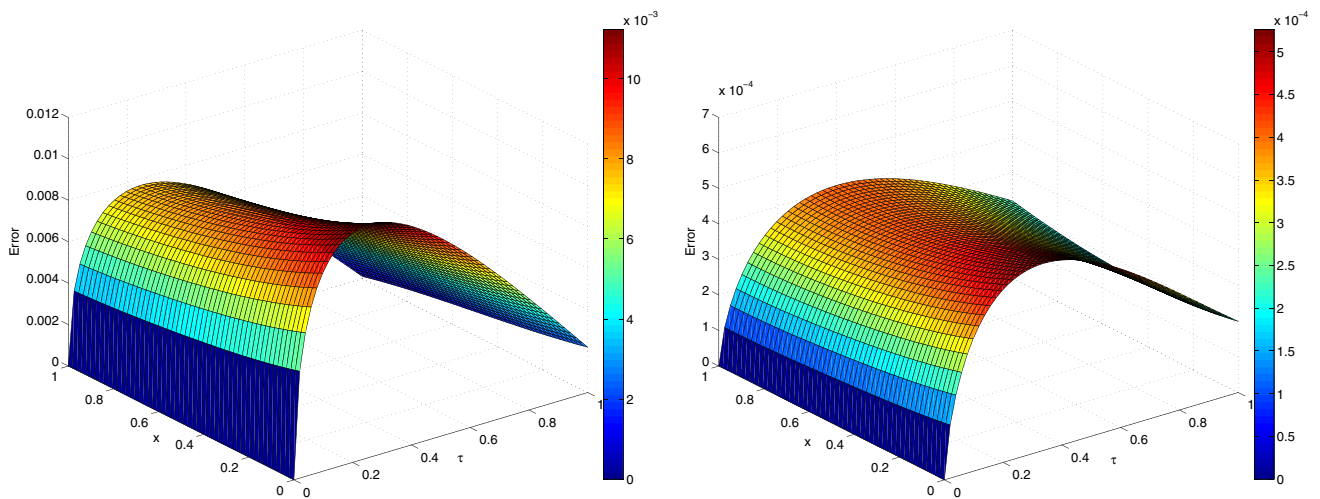


Fig. 4 The AE for the proposed method with $m_1 = 3, m_2 = 4, \theta = 0.76$ (left side) and $\theta = 0.87$ (right side) for Example 2

Table 4 The runtime (in seconds) of the proposed method with different choices of m_1 and m_2 for Example 2

case	m_1	m_2	CPU times
1	3	3	17.54
2	3	4	19.80
3	4	4	24.61
4	5	4	27.19
5	5	5	31.53

m_1 and m_2 are reported in Table 4. Table 3 as well as Figs. 3 and 4 are suggestive of an acceptable accuracy of the proposed method for approximate solutions of the proposed problem.

6 Conclusion

In this paper, we proposed an optimization technique based on GLPs coupled with Lagrange multipliers for the study of FGT. The scheme was applied to two test problems and the results were recorded in related tabular and graphical forms. From Figs. 1, 2, 3 and 4, and Tables 1 and 3, we verify that only a few number of basis functions are needed in the GLPs method to obtain a satisfactory result. The results of our algorithm pave the way for conducting further research on similar problems in this field to improve theoretical analysis and practical performance of algorithms and achieve additional results in future. In our future works, our new

method can be applied to other nonlinear partial differential equations such as fractional diffusion-wave equation, fractional telegraph equation, fractional Klein–Gordon equation, and fractional optimal control problems. Finally, from the numerical results, the biological behavior of the tumor is predicted and the theoretical statements are justified.

Funding The authors have not disclosed any funding.

Declarations

Conflict of interest The authors declare that they have no conflict of interest.

References

- Abo-Gabal H, Zaky MA, Doha EH (2022) Fractional Romanovski–Jacobi tau method for time-fractional partial differential equations with nonsmooth solutions. *Appl Numer Math* 182:214–234
- Agrawal OP, Machado JAT, Sabatier J (2004) *Nonlinear dynamics. Fractional derivatives and their applications*, Kluwer Academic Publishers, Special Issue
- Aizenshtadt VS, Krylov VI, Metel’skii AS (1966) *Tables of Laguerre polynomials and functions*. Mathematical tables series. Pergamon Press, Oxford
- Alififeris C, Trafalis DT (2015) Glioblastoma multiform: Pathogenesis and treatment. *Pharmacol Ther* 152:63–82
- Bavi O, Hosseininia M, Heydari MH, Bavi N (2022) SARS-CoV-2 rate of spread in and across tissue, groundwater and soil: a meshless algorithm for the fractional diffusion equation. *Eng Anal Boundary Elem* 138:108–117
- Bhrawy AH, Alhamed YA, Baleanu D, Al-Zahrani AA (2014) New spectral techniques for systems of fractional differential equations using fractional-order generalized Laguerre orthogonal functions. *Fract Calc Appl Anal* 17:1137–1157
- Bhrawy AH, Alhamed YA, Baleanu D, Al-Zahrani AA (2014) New spectral techniques for systems of fractional differential equations using fractional-order generalized Laguerre orthogonal functions. *Fract Calc Appl Anal* 17:1137–1157
- Blissitt PA (2014) Clinical practice guideline series update: care of the adult patient with a brain tumor. *J Neurosci Nurs* 46(6):367–8
- Chen Y, Yu H, Meng X, Xie X, Hou M, Chevallier J (2021) Numerical solving of the generalized Black–Scholes differential equation using Laguerre neural network. *Digital Signal Process* 112:103003. <https://doi.org/10.1016/j.dsp.2021.103003>
- Chi X, Jiang X (2021) Finite difference Laguerre–Legendre spectral method for the two-dimensional generalized Oldroyd-B fluid on a semi-infinite domain. *Appl Math Comput* 402:126138. <https://doi.org/10.1016/j.amc.2021.126138>
- Cong ND, Tuan HT, Trinh H (2020) On asymptotic properties of solutions to fractional differential equations. *J Math Anal Appl* 484(2):123759
- Cruywagen GC, Woodward DE, Tracqui P, Bartoo GT, Murray JD, Alvord EC Jr (1995) The modeling of diffusive tumours. *J Biol Syst* 3(4):937–45
- Daşcıoğlu A, Varol D (2021) Laguerre polynomial solutions of linear fractional integro-differential equations. *Math Sci* 15:47–54
- Ellor SV, Pagano-Young TA, Avgeropoulos NG (2014) Glioblastoma: background, standard treatment paradigms, and supportive care considerations. *J. Law Med. Ethics.* 42(2):171–182
- Garrappa R, Kaslik E (2020) On initial conditions for fractional delay differential equations. *Commun Nonlinear Sci Numer Simul* 90:105359
- Hajimohammadi Z, Parand K (2021) Numerical learning approximation of time-fractional sub diffusion model on a semi-infinite domain. *Chaos Solitons Fractals* 142:110435. <https://doi.org/10.1016/j.chaos.2020.110435>
- Hajiseyedazizi SN, Samei ME, Alzabut J, Chu Y-M (2021) On multistep methods for singular fractional q-integro-differential equations. *Open Math.* 19(1):1378–1405
- Hammad HA, Agarwal P, Momani S, Alsharari F (2021) Solving a fractional-order differential equation using rational symmetric contraction mappings. *Fractal Fract.* 5(4):159. <https://doi.org/10.3390/fractalfract5040159>
- Hassani H, Avazzadeh Z, Tenreiro Machado JA (2020) Numerical approach for solving variable-order space-time fractional telegraph equation using transcendental Bernstein series. *Eng Comput* 36:867–878
- Hassani H, Avazzadeh Z, Tenreiro Machado JA, Agarwal P, Bakhtiar M (2022) Optimal solution of a fractional HIV/AIDS epidemic mathematical model. *J Comput Biol* 29(3):276–291
- Hassani H, Tenreiro Machado JA, Avazzadeh Z (2019) An effective numerical method for solving nonlinear variable-order fractional functional boundary value problems through optimization technique. *Nonlinear Dyn* 97:2041–2054
- He Z-Y, Abbes A, Jahanshahi H, Alotaibi ND, Wang Y (2022) Fractional order discrete-time SIR epidemic model with vaccination: Chaos and complexity. *Mathematics* 10(2):165
- Heydari MH, Atangana A (2022) A numerical method for nonlinear fractional reaction-advection-diffusion equation with piecewise fractional derivative. *Math Sci* <https://doi.org/10.1007/s40096-021-00451-z>
- Heydari MH, Hooshmandasl MR, Maalek Ghaini FM (2014) An efficient computational method for solving fractional biharmonic equation. *Comput Math Appl* 68(3):269–287
- Hosseininia M, Heydari MH (2019) Meshfree moving least squares method for nonlinear variable-order time fractional 2D telegraph equation involving Mittag-Leffler non-singular kernel. *Chaos Solitons Fractals* 127:389–399
- Hussien HSh (2019) Efficient collocation operational matrix method for delay differential equations of fractional order. *Iran J Sci Technol Trans A. Sci* 43:1841–1850
- Hussien HSh (2019) Efficient collocation operational matrix method for delay differential equations of fractional order. *Iran J Sci Technol Trans A Sci* 43:1841–1850
- Jaros J, Kusano T (2014) On strongly monotone solutions of a class of cyclic systems of nonlinear differential equations. *J Math Anal Appl* 417:996–1017
- Johnson DR, Fogh SE, Giannini C, Kaufmann TJ, Raghunathan A, Theodosopoulos PV, Clarke JL (2015) Case-based review: Newly diagnosed glioblastoma. *Neurooncol Pract.* 2(3):106–121
- Karthikeyan K, Karthikeyan P, Baskonus HM, Venkatachalam K, Chu YM (2021) Almost sectorial operators on ψ -Hilfer derivative fractional impulsive integro - differential equations. *Math. Methods Appl. Sci.* 1-15
- Kreyszig E (1978) *Introductory functional analysis with applications*. Wiley, Berlin
- Kumar M, Upadhyay S, Rai KN (2018) A study of lung cancer using Modified Legendre wavelet Galerkin method. *J Therm Biol* 78:356–366
- Lorenzo CF, Hartley TT (2000) Initialized fractional calculus. *Int J Appl Math* 3(3):249–265

- Nelson SJ, Cha S (2003) Imaging glioblastoma multiforme. *Cancer J* 9(2):134–145
- Odibat Z (2019) On the optimal selection of the linear operator and the initial approximation in the application of the homotopy analysis method to nonlinear fractional differential equations. *Appl Numer Math* 137:203–212
- Perry J, Zinman L, Chambers A, Spithoff K, Lloyd N, Laperriere N (2006) The use of prophylactic anticonvulsants in patients with brain tumours—a systematic review. *Curr Oncol* 13(6):222–229
- Phillips HS, Kharbanda S, Chen R, Forrest WF, Soriano RH, Wu TD, Misra A, Nigro JM, Colman H, Soroceanu L, Williams PM, Modrusan Z, Feuerstein BG, Aldape K (2006) Molecular subclasses of high-grade glioma predict prognosis, delineate a pattern of disease progression, and resemble stages in neurogenesis. *Cancer Cell* 9(3):157–173
- Podlubny I (1999) *Fractional differential equations*. Academic Press, New York
- Radmanesh M, Ebadi MJ (2020) A local mesh-less collocation method for solving a class of time-dependent fractional integral equations: 2D fractional evolution equation. *Eng Anal Boundary Elem* 113:372–381
- Rashid S, Sultana S, Karaca Y, Khalid A, Chu Y-M (2022) Some further extensions considering discrete proportional fractional operators. *Fractals* 30(1):2240026
- Roohi R, Heydari MH, Bavi O, Emdad H (2021) Chebyshev polynomials for generalized Couette flow of fractional Jeffrey nanofluid subjected to several thermochemical effects. *Eng Comput* 37:579–595
- S. Rashid, E. I. Abouelmagd, A. Khalid, F. B. Farooq, Y. -M. Chu, Some recent developments on dynamical h-discrete fractional type inequalities in the frame of nonsingular and nonlocal kernels. *Fractals*,30 (2) 2240110 (2022)
- Sabermahani S, Ordokhani Y, Lima PM (2020) A novel lagrange operational matrix and tau-collocation method for solving variable-order fractional differential equations. *Iran J Sci Technol Trans A Sci* 44:127–135
- Shahni J, Singh R (2022) Numerical simulation of Emden-Fowler integral equation with Green's function type kernel by Gegenbauer-wavelet, Taylor-wavelet and Laguerre-wavelet collocation methods. *Math Comput Simul* 194:430–444
- Shiralashetti, S. C. Kumbinarasaiah S (2020) Laguerre wavelets exact parseval frame-based numerical method for the solution of system of differential equations, *Int J Appl Comput Math* <https://doi.org/10.1007/s40819-020-00848-9>
- Singh R, Rehman AU, Masud M, Alhumyani HA, Mahajan S, Pandit AK, Agarwal P (2022) Fractional order modeling and analysis of dynamics of stem cell differentiation in complex network. *AIMS Math* 7(4):5175–5198
- Singla K (2021) Existence of series solutions for certain nonlinear systems of time fractional partial differential equations. *J Geom Phys* 167:104301
- Sun H, Chen W, Wei H, Chen Y (2011) A comparative study of constant-order and variable-order fractional models in characterizing memory property of systems. *Eur Phys J Spec Top* 193:185–192
- Thakkar JP, Dolecek TA, Horbinski C, Ostrom QT, Lightner DD, Barnholtz-Sloan JS, Villano JL (2014) Epidemiologic and molecular prognostic review of glioblastoma. *Cancer Epidemiol Biomark Prev* 23(10):1985–1996
- Tracqui P, Cruywagen GC, Woodward DE, Bartoo GT, Murray JD, Alvord EC Jr (1995) A mathematical model of glioma growth: the effect of chemotherapy on spatio-temporal growth. *Cell Prolif* 28(1):17–31
- Urbańska K, Sokołowska J, Szmidi M, Sysa P (2014) Glioblastoma multiforme - an overview. *Contemp Oncol (Pozn)*. 18(5):307–312
- Vargas AM (2022) Finite difference method for solving fractional differential equations at irregular meshes. *Math Comput Simul* 193:204–216
- Wang F-Z, Khan MN, Ahmad I, Ahmad H, Abu-Zinadah H, Chu Y-M (2022) Numerical solution of traveling waves in chemical kinetics: time-fractional fishers equations. *Fractals* 30(2):22400051
- Woodward DE, Cook J, Tracqui P, Cruywagen GC, Murray JD, Alvord EC Jr (1996) A mathematical model of glioma growth: the effect of extent of surgical resection. *Cell Prolif* 29(6):269–288
- Xu Y, Zhang Y, Zhao J (2019) Error analysis of the Legendre-Gauss collocation methods for the nonlinear distributed-order fractional differential equation. *Appl Numer Math* 142:122–138
- Yu H, Wu B, Zhang D (2019) The Laguerre-Hermite spectral methods for the time-fractional sub-diffusion equations on unbounded domains. *Numer Algorithms* 82:1221–1250
- Z. Abdollahi M, Mohseni Moghadam H, Saeedi MJ, Ebadi A (2021) computational approach for solving fractional Volterra integral equations based on two dimensional Haar wavelet method. *Int J Comput Math*. <https://doi.org/10.1080/00207160.2021.1983549>
- Zaky MA (2019) Recovery of high order accuracy in Jacobi spectral collocation methods for fractional terminal value problems with non-smooth solutions. *J Comput Appl Math* 357:103–122
- Zaky MA (2020) An accurate spectral collocation method for nonlinear systems of fractional differential equations and related integral equations with nonsmooth solutions. *Appl Numer Math* 154:205–222
- Zhang D, Miao X (2017) New unconditionally stable scheme for telegraph equation based on weighted Laguerre polynomials. *Numer Methods Partial Differ Equ* 33(5):1603–1615

Springer Nature or its licensor (e.g. a society or other partner) holds exclusive rights to this article under a publishing agreement with the author(s) or other rightsholder(s); author self-archiving of the accepted manuscript version of this article is solely governed by the terms of such publishing agreement and applicable law.